2019

Design, Synthesis and Characterization of Biomimetic, Bioinspired and Bio-related Functional Polymers for Atmospheric Water Recovery

Abdullah Alqassar
University of Central Florida

DESIGN, SYNTHESIS AND CHARACTERIZATION OF BIOMIMIERIC, BIOINSPIRED AND BIO-RELATED FUNCTIONAL POLYMERS FOR ATMOSPHERIC WATER RECOVERY

by

ABDULLAH ALQASSAR

B.S. WILKES UNIVERSITY

A thesis submitted in partial fulfullment of the requirments
for degree of Master Science in Environmental Engineering
in the Department of Civil, Environmental and Construction Engineering
in the College of Engineering and Computer Science
at University of Central Florida
Orlando, Florida

Fall Term

2019

Major Professor: Ni-Bin Chang

ABSTRACT

Atmospheric water recovery in changing environments has received wide attention in environmental science and engineering communities due to rapid population growth and frequent droughts. This study is focused on the design, synthesis, and characterization of biomimetic, bioinspired, and bio-related functional polymers (b^3p) to help resolve the water supply issue especially in arid or semi-arid regions. It is aimed to develop unique synthetic methods to access well-defined polymers with the aid of nanomaterials and metal to produce next generation polymer materials for better atmospheric water recovery. The design of such new b^3p is bioinspired by some skin materials of biological species such as frogs, beetles, or spiders. Such synthetic efforts are also coupled with fundamental studies of the polymer functions and structures, providing renewed understanding of how molecular structure and processing parameters associated with different nanomaterials impact macroscopic properties. This research was conducted by using a class of cross-linked hydrophilic copolymers known as hydrogels that exhibit a high fluid absorbency, up to 1,000 times to their own weight. Using free radical polymerization to cross-link two different monomers, such as Acrylamide (Am) and Acrylic Acid (Aa) loaded with Calcium Chloride ($CaCl_2$) and coated with gold nanoparticles (Au-Np's), can produce novel thermally-responsive hydrophilic copolymer (e.g. Poly (Am-co-Aa)/Au-Np's/$CaCl_2$) that was placed inside a controlled structure for testing. The new b^3p materials can adsorb water vapor in the evening via a swelling process and discharge water vapor in the morning via a deswelling process to harvest the atmospheric water for recovery and reuse. The new b^3p materials demonstrated high average swelling percentage of about 3541% when placed in water under a temperature range of [20-30^oC] for 5 hours. The hydrogel loaded with 3.3701

grams $CaCl_2$ was placed in the furnace under relative humidity percentage (RH) range of [80-90%] and can absorb up to 27% of the atmospheric water undergoing the same time. The research concludes that the proposed synthetic method contributes to solving such contemporary challenge in green chemistry to some extent. Further studies are needed to deeply investigate the ability of this new hydrogel to load more dissolved solids such as $CaCl_2$.

ACKNOWLEDGMENTS

I would like to deeply thank Dr. Ni-Bin Chang for advising me within this research project and the committee members Dr. Lei Zhai and Dr. Lorraine Leon for advising me as the thesis committee members. Dr. Zhai working with NanoScience Technology Center at Universality of Central Florida (UCF) helped part of the research by allowing me to work in his nanomaterial laboratory with the aid of especially his student, Ms. Sajia Afrin. Dr. Lorraine Leon who is a faculty with the Department of Martials Science and Engineering at UCF taught me the knowledge of Polymer Science and Engineering. Dr. Linan An working with Department of Material Sciences and Engineering at UCF allowed me to work in his laboratory using the furnace and Dr. Sakthivel in his team helped me with the laboratory operation and gave me access to the equipment. Mrs. Melissa Saint James who is the laboratory manager at Department of Civil, Environmental, and Construction Engineering helped me set up my experiment.

TABLE OF CONTENTS

.

LIST OF FIGURES

LIST OF TABLES

CHAPTER 1 INTRODUCTION

1.1 Background and motivations

Due to climate change impact and global economic development, human society is now facing more natural hazards and extreme weather such as droughts and water scarcity. A possible water scarcity will be faced by 2025 according to the United Nations (UN) [1]. Water is the most fundamental natural resources for life support. Rapid urbanization can lead to food, energy and water scarcity and trigger more demand for water consumption over different scale and time. According to the United States Geological Survey (USGS), planet earth is covered with 71% water in which 96.5% in oceans, 0.9% in other saline water and just 2.5% is freshwater where 3% of that can be found in the atmosphere [2].This study is dedicated for seeking a novel solution for solving the water scarcity issue in response to sustainable development goals promoted by (UN).

Atmospheric water can be found as liquid in rainfall or drops, and as a solid in snowfall and hails. Earth contain small amount of atmospheric water when compared to other natural resources however, this kind of water plays an important role in the hydrologic cycle and it's mandatory for several creatures; for example, atmospheric water is a fundamental source of water to amphibians such as frogs that can adapt to the harshest environments using their most extraordinary survival strategies utilizing moisture from airflow. All airflow on earth contains some moisture that can frogs use by condensing it on their skins using natural strategical techniques to cool down their skin temperature.

An artificial atmospheric water harvesting technique can be inspired by these species. Also, it can be synthesized and characterized using polymer science and engineering principle to help us

produce biomimetic, bioinspired, and bio-related functional polymers (b^3p) economically and environmentally. The obtained freshwater could be applied for drinking, irrigation or other applications. This is especially true in the regions that desalinated water is the major potable source. State of Florida has several water resources such as groundwater or rivers however; desalinated water that is obtained from seawater is critical in some regions, such as Tampa Bay. Even though cost for desalination went down over the years due to the treatment efficiency improvement, it is still not cost effective compared to other conventional treatment technologies. Tampa Bay desalination plant treats 250 MGD of seawater where it costs $3 per 1000 gallon according to South Florida Water Management District [3] in addition to the environmental impacts such as salty concentrate discharge and the enormous amount of energy consumed through the Reverse Osmosis (RO) operation that leads to indirect air pollution.

Atmospheric water can be captured by understanding couple of concepts such as relative humidity (RH), actual vapor pressure (e) and saturation vapor pressure (e_s) (see Equation 1) [4].

$$RH(\%) = \frac{e}{e_s} \tag{1}$$

RH is the measurement of moisture present in air and it is the ratio of e to e_s. The e is the pressure of water vapor exerted on a surface and the e_s is the vapor pressure at maximum moisture content that air can hold at a specific temperature. Therefore, when air temperature is saturated with vapor pressure, the temperature allowing this vapor to be condensed is called dew point temperature (T_d) where water will condense at T_d because the water in air is in equilibrium with liquid water; so, at or below this temperature, water must start to condense. Florida has a yearly average RH of 85% in the morning and 60% in the evening [5].Therefore, this good range of RH can be utilized for promoting atmospheric water recovery for drinking, irrigation and

other applications. However, in some regions the RH is quite low compared to Florida; for example, in semi-arid regions such as State of Kuwait that is located in the Middle-East, the average RH can be as low as 40 %. In this case, atmospheric water can be used as a supplemental source of water for the desalination plant and reduce the cost and environmental impact. To meet the goal, suitable synthetic polymer can be used along with an application of covenantal treatment methods such as filtration for producing good water quality. Also, it can be used for irrigation or as a major source of water in arid regions to maintain life of people and wildlife.

1.2 Aims and scope

The objectives of this study are to 1) synthesize and characterize a hydrophilic thermo-responsive copolymer based on Acrylic acid (Aa) and Acrylamide (Am) monomers that will be synthesized in combination with gold nanoparticle's (Au-Np's) as new hydrogel with the aid of a deliquescent salt, and 2) test the new hydrogel in a control system mimicking the frog behavior in water collection. Hence, this thesis encompasses the following work, including synthesis of copolymer hydrogel via free radical solution polymerization of Acrylamide (Am) and Acrylic acid (Aa) as hydrophilic monomers along with Gold nanoparticles (Au Np's) as heat absorbent. The hydrogel water vapor swelling capacity will be tested under different environmental conditions. Also, the effect of adding Au Np's will be studied for a larger water recovery and better quality. The science questions include 1) Can the Acrylic acid (Aa) and Acrylamide (Am) monomers synthesized in combination with gold nanoparticle's (Au-Np's) perform better in terms of swelling and deswelling than the traditional hydrogel, 2) Can the atmospheric water recovery be better off in terms of cost-effectiveness due to the cross-linked polymer with salt addition? A summary flow chart of the research is shown in Figure 1.

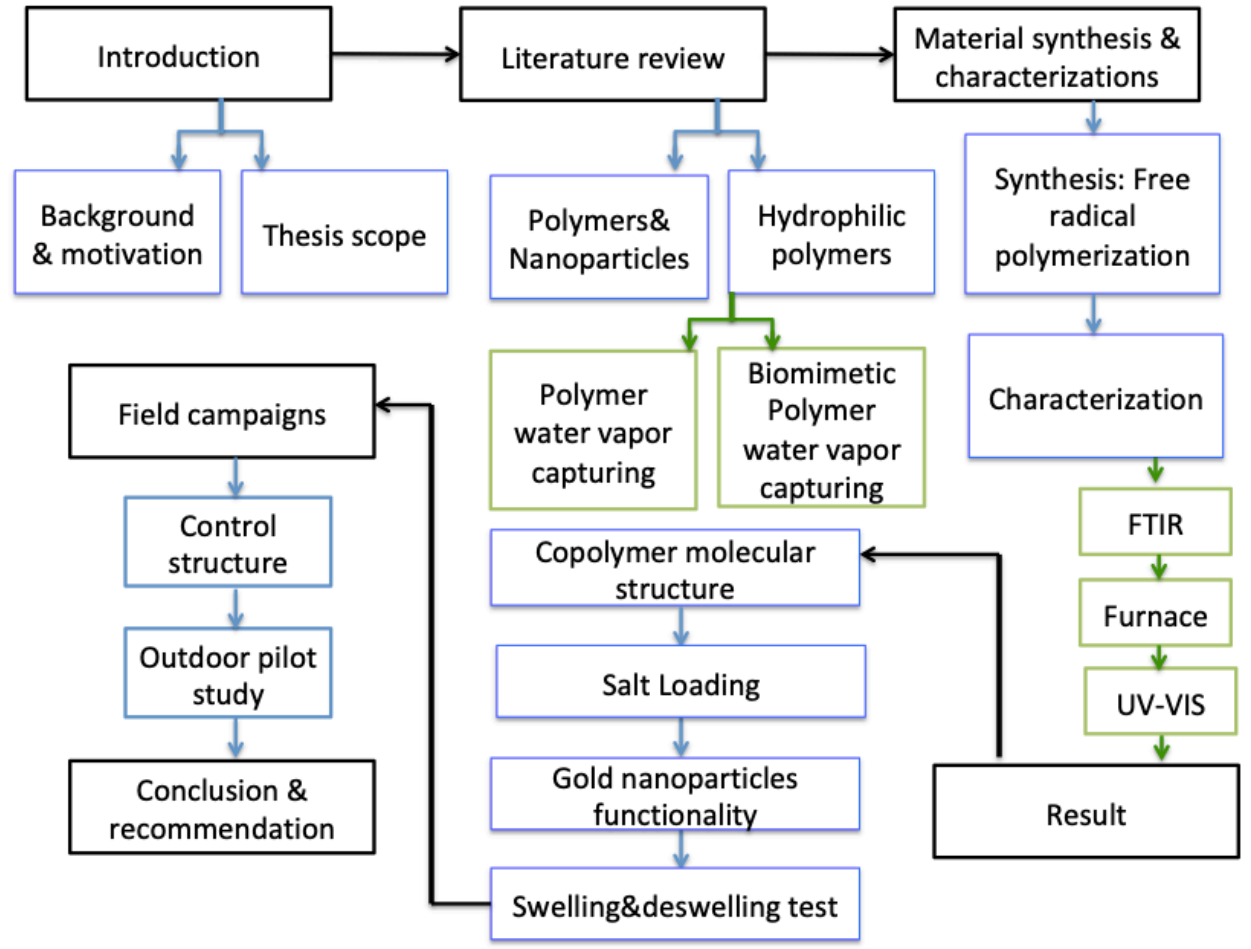

Figure 1 Research flowchart.

Chapter 1 indicates the problem statement mentioning human technological evolution and its effect on the ecological system. Also, the threatening condition of facing water scarcity in the future and offering a new technology for capturing Atmospheric Water (AW) to minimize this scarcity.

Chapter 2 will mention all remarkable literatures that invent atmospheric water capturing technology and introduce knowledge used from polymer science.

Chapter 3 detailed the experimental methodology, design and material needed as shown in the flowchart.

Chapter 4 interprets and discusses the data collected during the research. A conduction of an outdoor pilot study explained in Chapter 5. Finally, A general conclusion and recommendations for future work will be mentioned in Chapter 6.

CHAPTER 2 LITERATURE REVIEW

2.1 Polymers and nanoparticles

Polymers are group of repeated molecules and their repeating unit can be as high as 1000s [6]. As explained in the book of [7], currently polymers are contributing to our life in several aspects such as clothing, tools and weapons. In their early stages they were synthesized using natural materials such as natural rubber. Then by the time World War I took place and populations suffer lack of natural materials, scientist Leo Baekeland's firstly discovered 2,3-dimethylbutadiene (synthetic rubber) where it was produced and commercialized in 1910.

Up until this century, human discovered several polymerization techniques such as free radical polymerization that is dependent on three different stage. First, active center initiation stage that is achieved by homolytic scission and then electron transfer into or from a molecule or ion. After that, polymer chain propagation stage take place by monomer addition to the active center. Finally, when this stage ceases, termination stage predominates by destroying the active center. This type of polymerization can be categorized by 1) bulk polymerization where the reaction medium contains monomer and monomer soluble in initiator, 2) solution polymerization where the polymer, monomer and initiator are soluble in the solvent, 3) suspension polymerization where polymer, monomer and initiator should be insoluble in the reaction medium, or 4) emulsion polymerization where, polymer, monomer is insoluble, and the initiator is insoluble in the monomers but in the suspension medium.

Polymers can either be repeated by one functional group (Homo-Polymer) or two or more functional group (copolymer). The copolymers can be classified into different categories such as *block copolymer* where repeated units occur in long sequences, *alternating copolymer* where

repeated units are alternating sequentially, *graft copolymer* where the main chain have branches and *random copolymer* where repeated units are organized randomly (Figure 2).

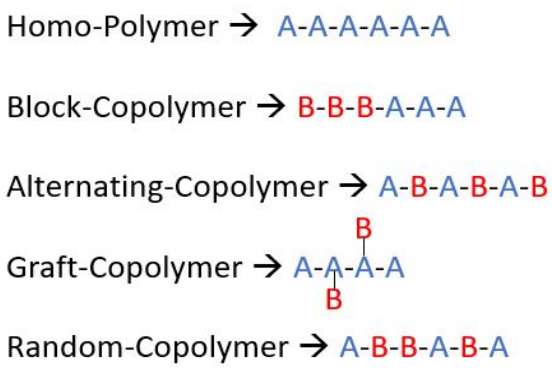

Figure 2 Polymers and copolymer classification. A-B different functional group.

A hydrogel is a 3D network structure that is stiffer than regular polymer and it is achieved by cross-linking a hydrophilic polymer. It can hold tremendous amount of water up to 500-1000 times its own weight. This phenomenon is controlled by pH, ionic strength, degree of cross-linking and temperature. As shown in (2) derived by [8], a high hydrophilic and ionic functional groups will result in high degree of swelling. Also, when there is low degree of cross-linking, concentration of ionic solution and polymer-solvent affinity the degree of swelling is high. Different functional groups show different swelling behavior when exposed to temperature because; it can affect the monomers hydrogen bonding. A hydrogel in regard with temperature can be categorized into negative temperature-sensitive polymers/hydrogels that expose a Low Critical Solution Temperature (LCST) behavior. These types of polymers swell at low temperature and deswell at high temperature. In contrast, other polymers/hydrogels expose positive temperature-sensitive polymers/hydrogels that shows Upper Critical Solution Temperature (UCST) which swell at high temperature and deswell at low temperature [9].

$$q_m^{5/3} = \frac{[\left(\frac{i}{2v_u\sqrt{s^*}}\right)^2 + (\frac{0.5 - x_1}{V_1})]}{(\frac{v_e}{v_o})} \quad (2)$$

where

$q_m^{5/3}$, Maximum degree of swelling

i, Charge per polymer unit in polyelectrolyte

v_u, Molecular volume of repeating unit

s^*, Solution ionic strength

x_1, Interaction free- energy per kT where K is Boltman's constant and T is the absolute temperature

v_e, Effective number of chains in the network

v_e, Volume of the relaxed Network charges per polymer unit in polyelectrolytes

Polymers can be reinforced by nanoparticles based on the type of application. For example, titanium dioxide (TiO_2) can be added to the polymer matrix to make it more hydrophilic. Also, carbon nanotubes (CNT) can be added to the polymer either for increasing heat absorption or to make the polymer more hydrophilic once they are functionalized with hydrophilic functional groups. Furthermore, gold or silver nanoparticles (Au Np's, Ag Np's) can be added to the polymer for increasing heat absorption or to encourage antimicrobial activity.

CNT has been used in variety of applications such as cement enforcement, heat conduction, and water collection. They are hydrophobic in nature and can be converted into hydrophilic by grafting oxygen functional groups on their surface [10]. Pinheiro et al. [11] preformed an

experiment on that and their result in water harvesting was promising when they placed hydrophilic CNT surface on hydrophobic CNT by having a vertical alignment of hydrophobic and hydrophilic CNT (VACNT) with the combination of polyethelyne, steel-screen and carbon felt. Their final product were organized as Polyethelyne/VACNT's/steel-screen/ /(superhydrophobic VACNT's/carbon fiber felt). Finally, they achieved 30 ($L/m^2/h$) of water at RH%=90. However, CNT are toxic and they are listed under Toxic Substance Control Act (TSCA) by the United State Environmental Protection Agency (US EPA) [12]. CNT can cause programed cell death once established above 400 micro/L [13]. A summary of CNT application in water collection is shown in Table 1.

Table 1 Carbon nanotubes application in water absorption.

Article title	Synthesis summary	Source
Vertically Aligned Super-Hydrophilic Carbon nanotube	-Vertically Aligned Carbon Nanotubes were synthesized by Thermal Chemical Vapor Deposition(TCVD) on 10 × 10 mm stainless steel screen and Carbon Fiber Felt (CFF) substrates. Oxygen functional groups grafted on VACNTs surface to changed them to super-hydrophilic. -Super-Hydrophobic VACNTs were functionalized in pure oxygen atmosphere into a Microwave Plasma (MWCVD) reactor at 800 W microwave power -Then the super-hydrophilic VANT were placed in a controlled system as: Polyethelyne/VACNT's/steel-screen/ /(superhydrophobic VACNT's/carbon fiber felt)	[14]
Vertically aligned multiwalled carbon nanotube forests (NTFs)	-NTFs were synthesized via water-assisted chemical vapor deposition (CVD) on a silica substrate. -The hydrophobic functionalized side of the NTF, 1H,1H,2H-heptadecafluoro-1-decene (HDFD; 99%, Sigma-Aldrich) was coated onto the top surface of the as-grown NTF and plasma treated (700 V direct current) for 2 min -The Hydrophilic functionalization on the opposite side of the NTF, 0.5 mL of poly(ethylene glycol) methacrylate (PEGMA) monomer (average Mn = 360; Sigma-Aldrich) was coated onto the surface, and the NTF was plasma-treated (700 V direct current) for 2 min	[15]
Carbon Nanotubes immobilized-super absorbing polymer (CNIM – SAP)	-The super-absorbing polymer binds strongly to water and generates water clusters -The CNTs are operable to interrupt the specific water polymer and water -water interactions to generate more free water which permeates more easily through the membrane	[16]

There are several different nanoparticles that show very good heat absorption and can be mixed with polymer to make it a thermally responsive such as silver, copper, and gold. For this project we will focus on gold nanoparticles (Au-Np's).

Au-Np's are currently used in several science and engineering fields because their advantage in high surface-volume ratio that makes them suitable for many biological, medical, and physical applications. In this study, we used Au-Np's in our copolymer matrix to enhance the reduction of microbial activities within their surrounding environments and perform as a heat absorbent simultaneously. According to [17], Au-Np's can inhibit the growth of some microbes such as S.aureus, E-coli, B.subtillis, and K.pneumonia by 75.2, 74.3, 68.5 and 71.9 percentage respectively. This is achieved because the area reduction caused by Au-Np's inhibits bacteria culture growth by collapsing tRNA binding and ATP activity reduction. These reasons can prove that it can be used as an antimicrobial agent when mixed with the polymer matrix. Also, it can alter the polymer temperature sensitivity as well as it can improve the polymer wavelength absorption [18], [19]. In general, gold is a conductive metal and its nanoparticles have better heat absorption and light scattering capacity compared to other materials in the same size because its collective oscillation of its conductive electron [18].

2.2 Hydrophilic polymers

2.2.1 Polymer water vapor capturing

Polymers consist of many repeated sub-molecules called monomers and once it is introduced to water and have hydrophilic properties it can be called hydrogel. These monomers play the major role in the properties of the polymer and determine whether the polymer may become hydrophilic or hydrophobic. In this research, we concentrate on the hydrophilic polymers that

can be used for water absorption and condensation. This method is being practiced and applied by scientists for atmospheric water harvesting. For example, [14] developed a water harvesting method using radiative cooling of Low Density Polyethylene foil and paint it with (TiO_2) and Barium Sulfate ($BaSO_4$). [20] developed polymers based on Metal Organic Framework (MOF) and they are metal ions linked by molecular species. MOF's are highly crystalline and water absorbing materials; for example, MOF-841 can absorb 640 $cm^3.g^{-1}$ at 90% RH and they are suited for large scale applications. However, MOF's in general are not cost effective. Also, a novel desiccant polymer was synthesized to capture water using Epoxy Porous Organic Polymer (ep-pop) 2D/3D that was combined via Diels-Alder cycloaddition and they have the functionality of epoxy group that is highly hydrophilic; however, they are highly reactive in acid or base conditions; thus, their linking is challenging. These materials have water absorbing capacity close to MOF's of approximately 400 $cm^3.g^{-1}$ at 90% RH [21]. On the other hand, [22] combine acrylamide monomers (Am) with Carboxylic acid functionalized Carbon Nanotubes (COOH-CNT's); then, they inserted a deliquescent salt $CaCl_2$ to finally get a hydrogel so-called (PAM-CNT- $CaCl_2$). This hydrogel can be placed in a controlled structure and can capture water at low relative humidity > 40 %. Their results show that when a quantity of 35g dry PAM-CNT- $CaCl_2$ hydrogel swelled with water vapor for 17 hours; then, it may be allowed for deswelling for 2.5 hours under sunlight to recover 20g atmospheric water. The technology in their hydrogel that the deliquescent salt can capture water by dissolving itself and form a solution where the hydrogel can store this water maintaining the deliquescent salt in a solid state continuously. They used $CaCl_2$ because it is not toxic salt, cheap and commercially available. Also, they compare the performance of their hydrogel with other water collecting materials and their hydrogel water collecting capacity was promising. The disadvantage on this polymer is due to the use of carbon

nanotubes, and as discussed earlier that they are toxic. Yet, they are cost effective in comparison with gold nanoparticles. A summary of the advantages of both Au-Np's and CNT's are listed in Table 2.

Table 2. Au-Np's and CNT comparison.

	Au-Np's	**CNT**
Heat absorption	Yes	Yes
Antimicrobial activity	Yes	No
Cost ($) **(www.sigmaaldrich.com)**	116 for 5nm	1,780 for 4-5nm COOH functionalized. D*L(0.5-1.5)

2.2.2 Biomimetic, bioinspired, bio related functional polymers (b^3p)

Biomimicry and bioinspiration is an engineering approach to invent sustainable designs that are inspired naturally [23]. It was practiced since human early stages for example, airplane invention that was inspired by birds [24]. However, scientists were ignoring the effects on the ecological system in their designs. The difference in our definition is that the design is linked to the ecological system through sustainable engineering design [25]. Therefore, once the principles of the natural design are applied through engineering design using human-friendly nanotechnology, b^3p is achieved.

In this research B^3p can be accommodated by considering the adaptation methods of a frog. By seeing that, it is impossible not to be impressed for example a frog can survive 6 months without rain in the northern Australia dessert. These types of frogs called **hylid frogs** (LitoriaandCyclorana) [26],[27]. There are several types of frog species [28] and in this project, we will focus on the hylid frogs. These species can collect water using ectothermic properties by entering warm or humid tree holes or burrows to cool their skin temperature below ambient temperature and eventually reach the dew point temperature (T_d); then, water will start to

condense on their skin [27]. After that, water will be absorbed and saved in its bladder [29], and by using these strategies, a frog can gain water up to 0.93% of its body mass [30]. A frog can avoid dehydration by secretion of lipids-like material by applying it on its skin and this technique can help it for water balance in addition to its skin texture and sculpturing (Figure 3,a) [31], [32]. Also, several scientists have been bio-inspired to synthesize a polymer that mimics creatures. For example, spider silk and beetle back shell. A Natural Spider silk can collect water from vapor and it had been artificially produced by fabricating uniform nylon into poly (methylmethacrylate)/N,N-d imethylformamide-ethanol (Figure 3,b) [15], [33]. Also, beetle back shell contain hydrophilic regions on a hydrophobic background where it has been mimicked [34]. They accomplished that by producing a super-hydrophobic surface using Polyallylamine hydrochloride (PAH)/ polyacrylic acid (PAA) and PAH/silica nanoparticles. On the other hand, for the hydrophilic surface they used PAA in water/ 2-propanol. Then, the hydrophilic surface is placed on the super-hydrophobic surface and water is being collected as a beetle does (Figure 3,c). These kink of creature can collect water passively from rain, dew, moisture, and fog [35]

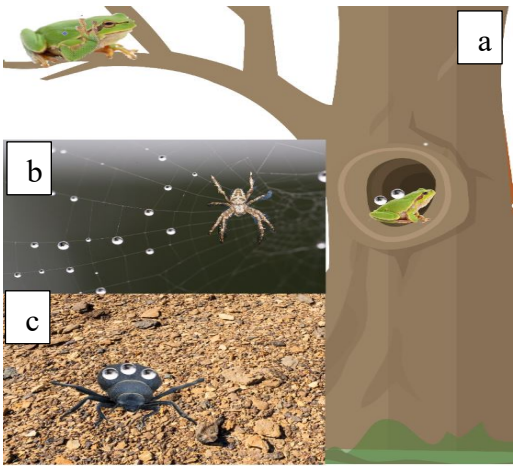

Figure 3 Creature behavioral atmospheric water recovery.

CHAPTER 3 METHODS FOR MATERIAL SYNTHESIS AND CHARACTARIZATIONS

3.1 Materials

Acrylamide suitable for electrophoresis (Am) >99% and acrylic acid as monomers, 5nm Gold Nanoparticles (Au Np's) improve heat absorbance and reduce antimicrobial activity, N,N'-Methylenebis(acrylamide) 99% as cross-linking agent, N,N,N'N'-Tetramethylenediamine (TEMED) 99% as cross-linking accelerator, potassium persulfate (KSP) as initiator. All chemicals were bought from Sigma-Aldrich without no further purification. WINGONEER ±5% humidity probe for monitoring the humidity in the furnace. Copper sheet metal as heat dissipater and water droplets induction were bought from amazon, Solar & battery fan were bought from Walmart to help accelerate the system heat dissipation caused by the copper plate. Edge glass microscope slides were bought from amazon to aim light entrance to the system. 2 plastic boxes were bought from SISTEMA Company.

3.2 Copolymer synthesis

3 glass vials were prepared each with 5mL nanopure water. In each vial 0.5 Am and Aa were added with 250 μL of Au Np's. Then, the dispersion was sonicated for 60 minutes to ensure homogenous mixing. After that, each vial was purged with argon for 15 minutes to remove dissolved oxygen. After that, 5mg KPS as an initiator, 0.38 mg MBAA cross-linking and 25 μL of TEMED as cross-linking accelerator were added to start the polymerization (Figure 4). The vials were placed in a silica gel oil path with controlled temperature between 60-70^{o}C for 3 hours to speed the polymerization kinetics. After completion, the polymers were rested at room temperature overnight and then placed in the freeze-dryer at -40^{o}C for 3 days to dry the hydrogel. After freeze-drying, one of the hydrogels were immersed in a deliquescent salt for 24 hours**.** The

resulted hydrogels are summarized in Table 3. The synthesis procedure was a combination between different methods in literatures ([22], [36], [37]).

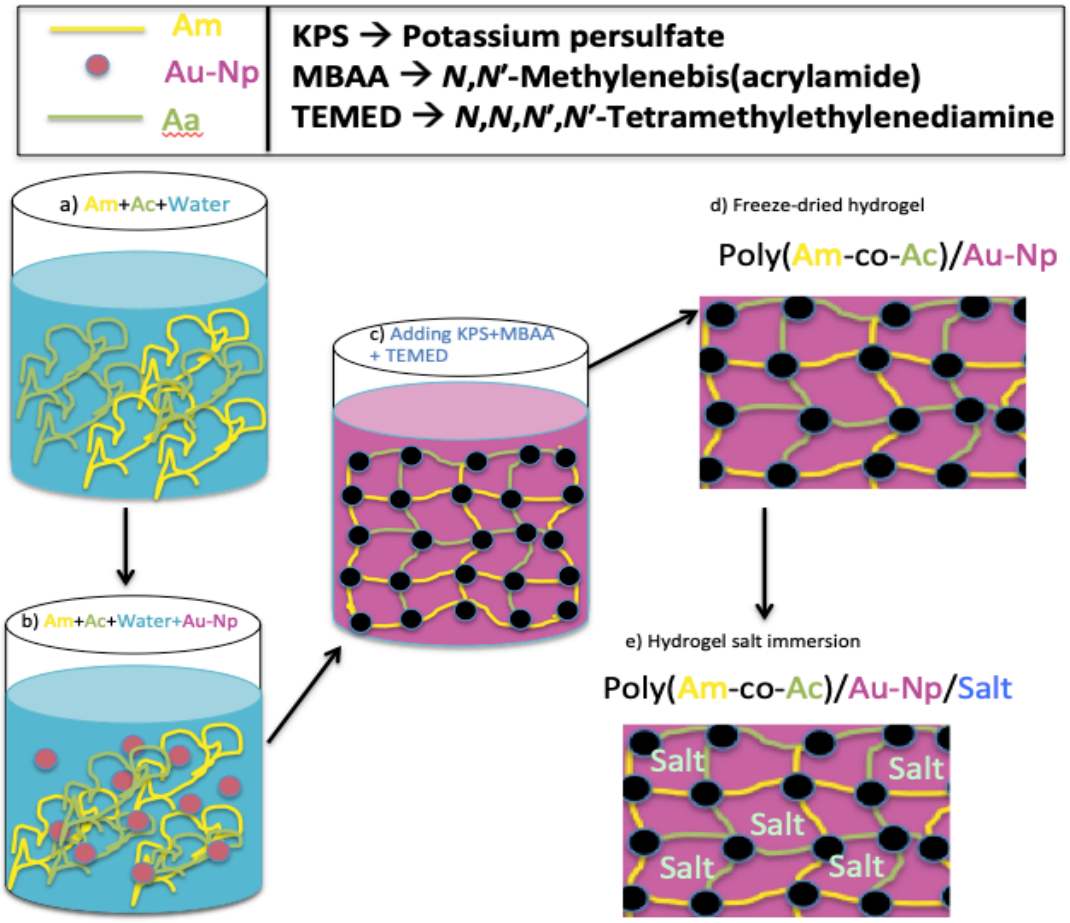

Figure 4 .Polymerization summary.

Table 3 Hydrogels summary.

Hydrogels	Deliquescent salt
P(Am-co-Aa)	-
P(Am-co-Aa)/Au Np's	-
P(Am-co-Aa)/Au Np's	0.4 $\frac{g}{mL}$ $CaCl_2$

3.3 Characterization

The characterization methods are a focal point in accomplishing a hydrogel that is suitable for the purpose of this project. FTIR will be used for confirming the copolymer functional group's bonding and the effect of adding Au-Np's on the bonding absorption peaks. The furnace will be used to assets the hydrogel swelling and deswelling temperature as well as the hydrogel swelling and deswelling behavior under different RH(%). SEM will be used to confirm the surface modifications by Au-Np's and TEM will help us to confirm the Au'Np's coating by the monomers. The UV-VIS will be used to see the effect of adding Au'Np's on the visible light absorption. Then, based on the characterization results, a controlled structure will be designed as an Atmospheric Water Generator that will aim in atmospheric water recovery (Figure 5)

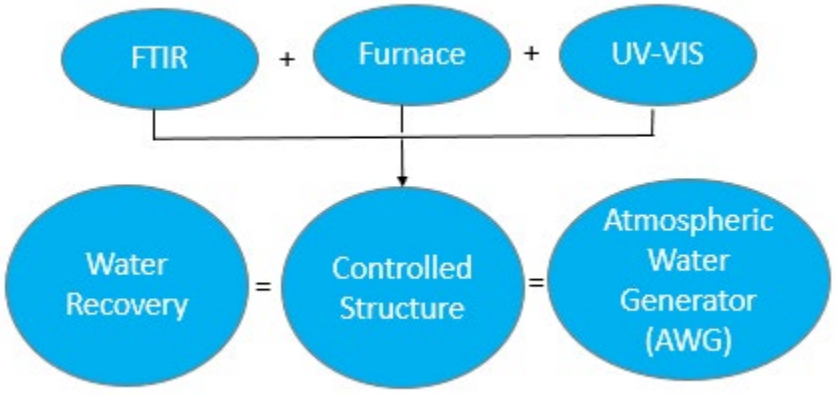

Figure 5 Characterization flow chart.

3.3.1 Fourier Transform Infrared (FTIR)

FT-IR Spectrometer-Shimadzu IRSpirit Eith QATR-SAT available at Nanosience Technology Center (NSTC) in University of Central Florida (UCF). The advantage of using this instrument is confirming the copolymer molecular structure. Different molecules absorb different

wavelength. When the sample is placed on FTIR, it undergoes IR radiation were some of it will be absorbed and some will not. Therefore, the functionality of it is to confirm the molecular structure of the hydrogel. Different FTIR readings were gathered from the literature for comparison with our produced copolymer (see Table 4).

Table 4 Literature FTIR bond stretching summary.

Source	[38]	[36]
Polymer	P(Am-co-Aa)	P(Am-co-Aa)
Monomer ratio	60:40	50:50
Polymerization	Radical	Radical
Bond Stretching/Units	cm^{-1}	%T Vs cm^{-1}
NH		3436-3425
OH		3650
OH&NH	3500	
CH		1973-2930
Asymmetrical CH	2900	
Symmetrical CH	2740	
C=O (AA)		1719-1705
C=O (Am)		1652-1690
C=O	1742	
Asymmetrical COO	1580	
Symmetrical COO	1448	
C=C (AA)		1630
C=C (Am)		1648
C-N (Cross-linker)	2186	1451-1407

3.3.2 Furnace

GSL1100X Tube Furnace-MTI Corporations at Advanced Material Processing and Analysis Center (AMPAC) at UCF will be used for testing the hydrogel behavior under different

temperatures and different RH(%). This can be done by connecting a dry and wet stream from a nitrogen cylinder and each of the streams will be controlled by valve. The humidity will be monitored by a humidity-sensor (see Figure 6). A schematic of the furnace layout is explained in Figure 7.

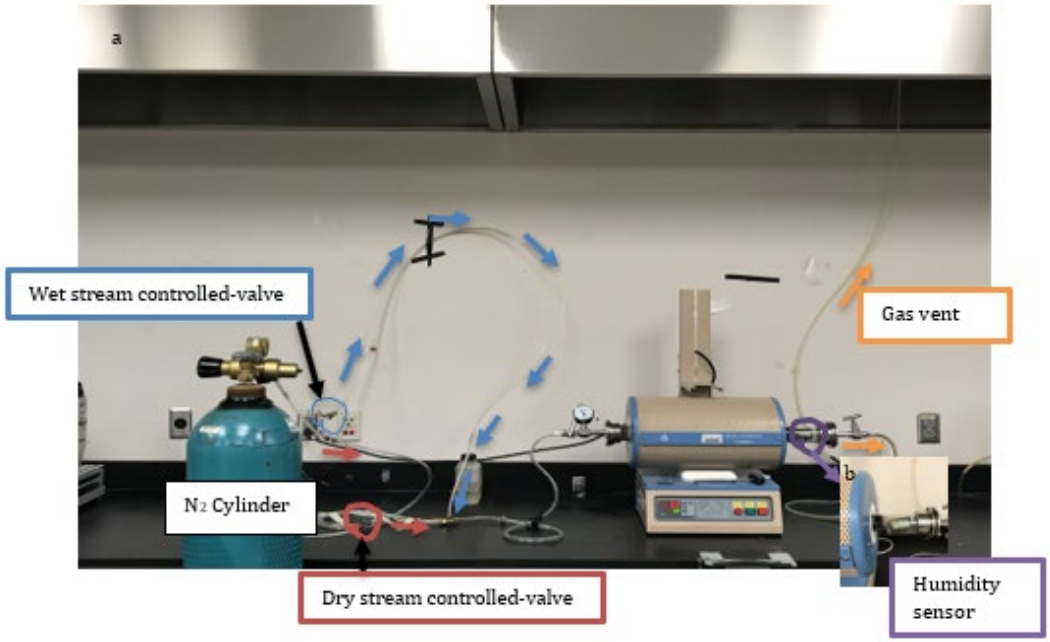

Figure 6 a) Furnace setup, b) zoom-in humidity sensor picture.

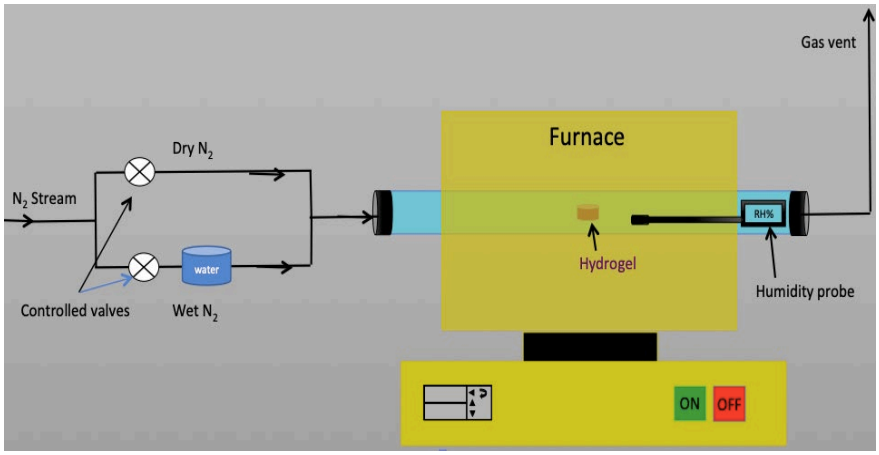

Figure 7. Schematic furnace setup.

3.3.3 Ultra Violet-Visible Light Spectrometer (UV-VIS)

Hach-Lange DR5000 UV-VIS Spectrometer at UCF Engineering 2 building lab 433. This equipment provide energy to the sample therefore, the sample structure will be analyzed based on the absorbed energy. Thus, it will be used to assess the effect of adding gold nanoparticles to the polymer matrix.

CHAPTER 4 RESULTS AND DISCUSSION

4.1 Copolymer molecular structure

After the free radical polymerization ceases, both hydrogels were in cylindrical shape. The plain hydrogel shows a transparent color whereas the hydrogel functionated with Au-Np' shows a dark to violet color (see Figure 8). To confirm the copolymer molecular structure and surface modification by Au-Np's, FTIR spectra were performed. All obtained data agreed with the literatures expressed in Table 4. As shown in Figure 9, P(Am-co-Aa) formation is confirmed as a result of the bands such as O-H and N-H stretching from (3000-3500cm^{-1}), C-H stretching from (2800-2900 cm^{-1}), C=O connected to COOH at 1700cm^{-1}, COO stretching from (1400-1500 cm^{-1}), and weak band from the cross-linking agent at 2180 cm^{-1}. The surface modification achieved by the addition of Au-Np's is confirmed by the Figure in showing the same bands at approximately the same wavenumbers with higher absorption. For example, C=O connected to COOH band at 1700 cm^{-1} in the plain copolymer expose an absorption of approximately 0.06a.u. on the other hand, the modified copolymer at the same band shows an absorption of approximately 0.13a.u because the surface modification by Au-Np's that is causing more heat absorption. This is can be explained by the Surface Plasma Resonance Phenomena (SPR) exposed by Au-Np's [39], [40] and [41].

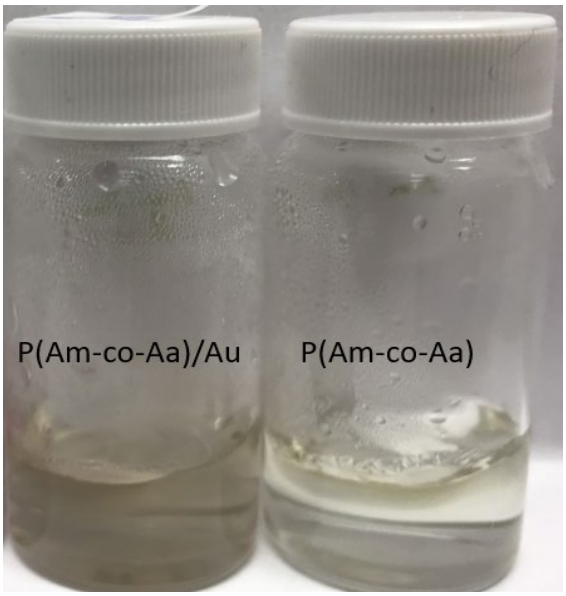

Figure 8 Hydrogel after polymerization.

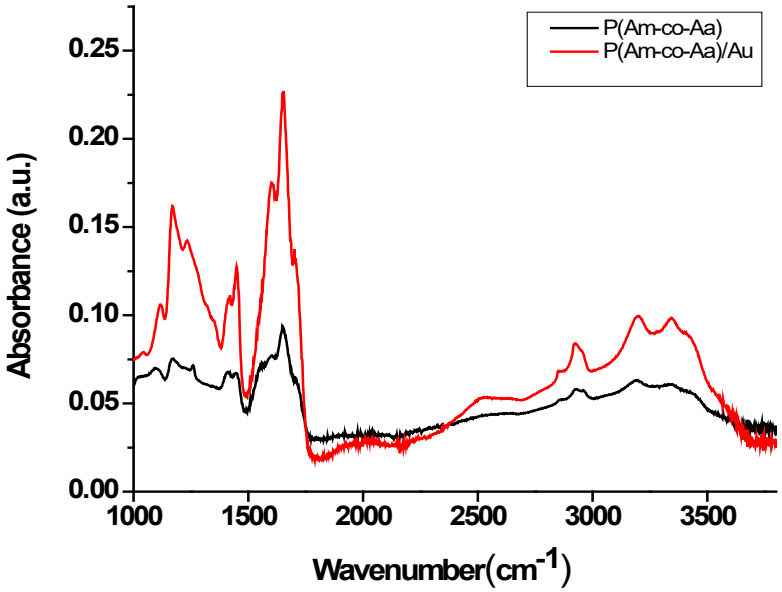

Figure 9 FTIR analysis for plain copolymer and copolymer with 250 μL Au-Np's.

As defined earlier, a copolymer is a polymer that contain two or more functional groups (see Figure 10a). They can be classified into different categories and in this research, we synthesize a random copolymer. Whenever this copolymer is hydrophilic and undergoes cross-linking, it become a hydrogel that shows a 3D network structure and more rigidity than uncross-linked copolymer (Figure 10b). In P(Am-co-Aa)/Au-np's/$CaCl_2$, the monomers were initiated by KPS in absence of oxygen to allow radical propagation and the reaction kinetics were catalyzed by applying heat. The repeated units are randomly distributed and connected by cross-linker MBAA were it was accelerated by TEMED.

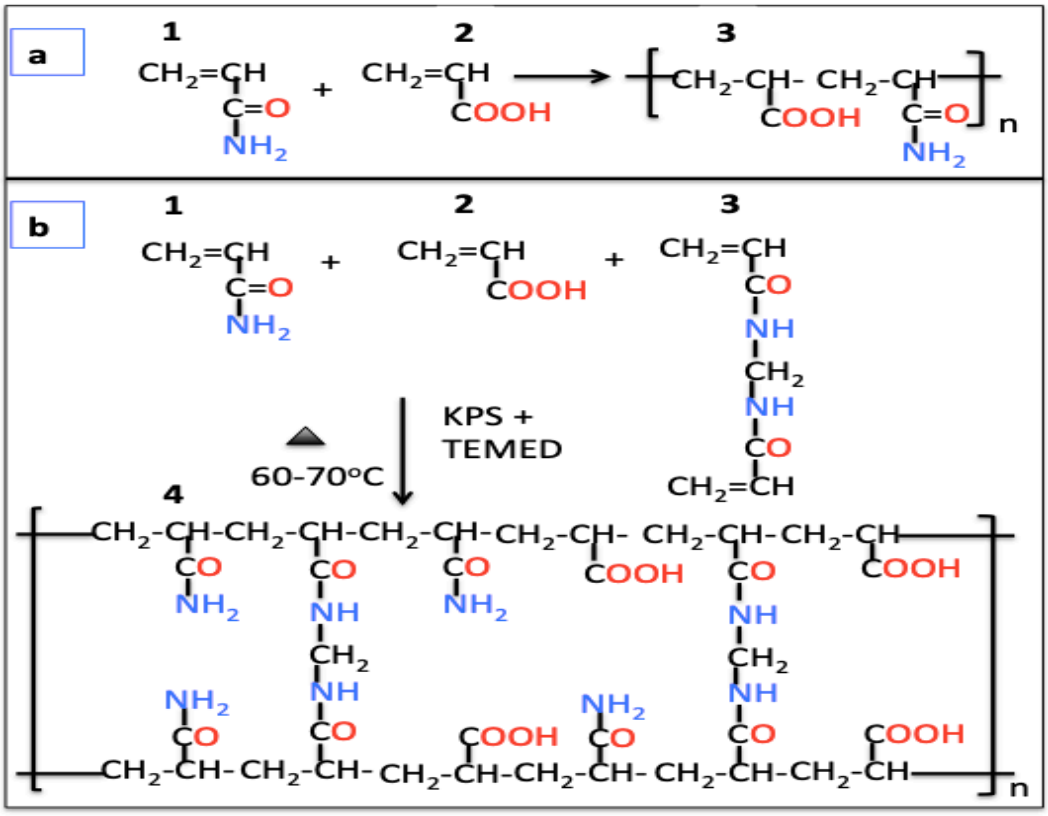

Figure 10 Possible hydrogel molecular structure. a1, b1) Acrylamide (Am). a2, b2) Acrylic acid (Aa), a3) P(Acrylamide-co-AcrylicAcid), P(Am-co-Aa). b3) N,N' Methylenebis (acrylamide)(MBAA).b4) cross-linked P(Am-co-Aa), Degree of polymerization (n), Potassium persulfate (KSP), N,N,N'N'-Tetramethylenediamine (TEMED).

4.2 Salt loading

After freeze-drying, the hydrogel were immersed in a 0.4$\frac{g}{mL}$ $CaCl_2$ at approximately pH=7 and temperature range of [20-30]ºC for 48 hours and the swelling was 521%. It was noticed that the swelling decreases in comparison to the hydrogel immersed in nanopure water. This is because the present of salt ions in the surrounding solution which are causing less osmotic pressure with the hydrogel. After completing the immersion step, the hydrogel was dried at 80ºC until constant weight is reached (4.4306 g). The weight difference was calculated to see the amount of salt loaded inside the polymer matrix and at the polymer surface that is 3.3701g (see Table 5). The hydrogel was washed to figure out the amount of the salt inside the polymer matrix and on its surface separately. The weight of the hydrogel after washing was 3.8625g therefore, the salt inside the polymer matrix is 2.802g and the rest is on the surface (0.899g). A summary of the synthesis method and possible final hydrogel structure is shown in Figure 11.

Table 5 P(Am-co-Aa)/Au immersed in 0.4 $\frac{g}{mL}$ $CaCl_2$ swelling

Dry weight (g)	1.0605	
Time (hours)	**Weight (g)**	**Swelling (%) (3)**
24	5.7506	442
48	6.5849	521

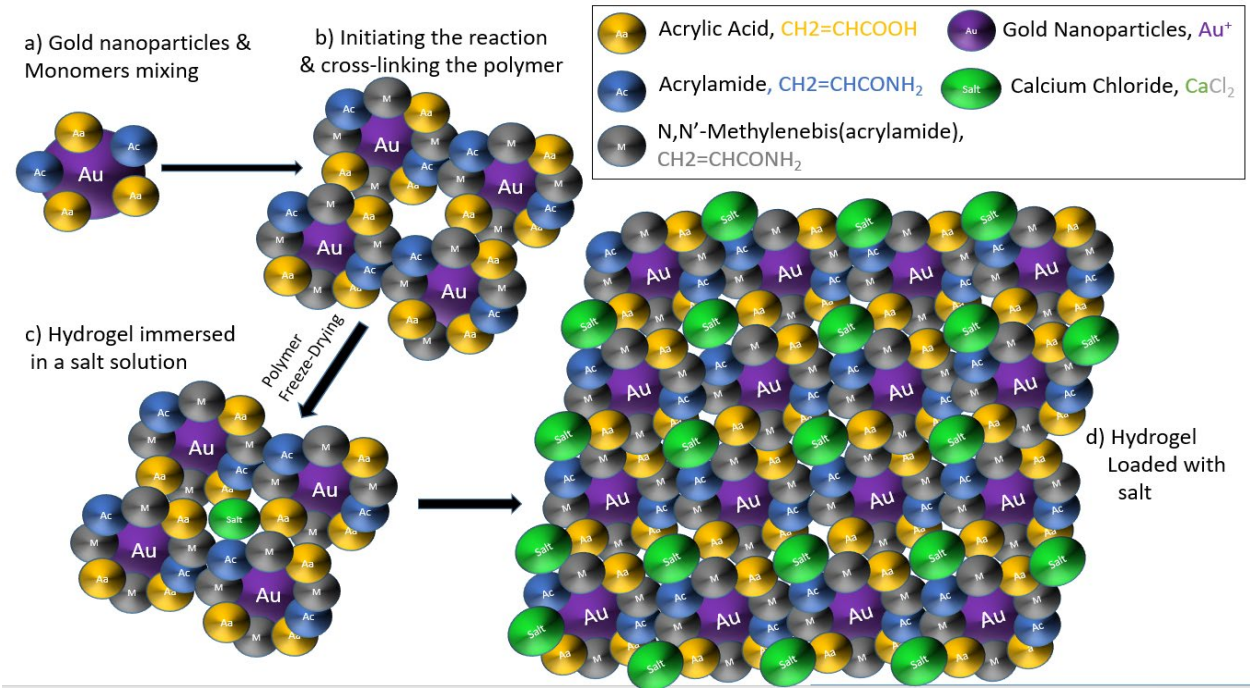

Figure 11 Possible hydrogel with salt loading.

4.3 Gold nanoparticles functionality

Plain Au exhibit 100% Visible light absorption at 526 nm (Figure 12) and, when it's diluted with nanopure water the absorption decreases to 5.7%. Pure solution of Am and AA is very weak in visible light absorption however, when just 250 μLAu Np's are added the visible light absorption increases. This is because the (SPR) resulting from the nanoparticles in the sample. This phenomenon can be defined as, when a metal nanoparticle is exposed to an electromagnetic field, a collective electron oscillation on the particle surface is activated causing high visible light absorption. Therefore, Figure 13 confirms that Au Np's can increase the VIS absorption by approximately 5.7% when added to the solution of Am and AA and the absorption peak shift to a lower frequency and higher wavelength 550nm, this shift is called red shift that is resulted from reduced electron density that confirms Au Np's surface modifications. Also, when Au is added to

the polymer mixture, the solution color changes from red into slightly violet color as a result from the increase in Au Np's diameter. This can be explained by the solution pH, which were around two. Hence, AA is partially protonated causing Au Np's bonding together and increasing in the particle size of the nanoparticles [19], [42].

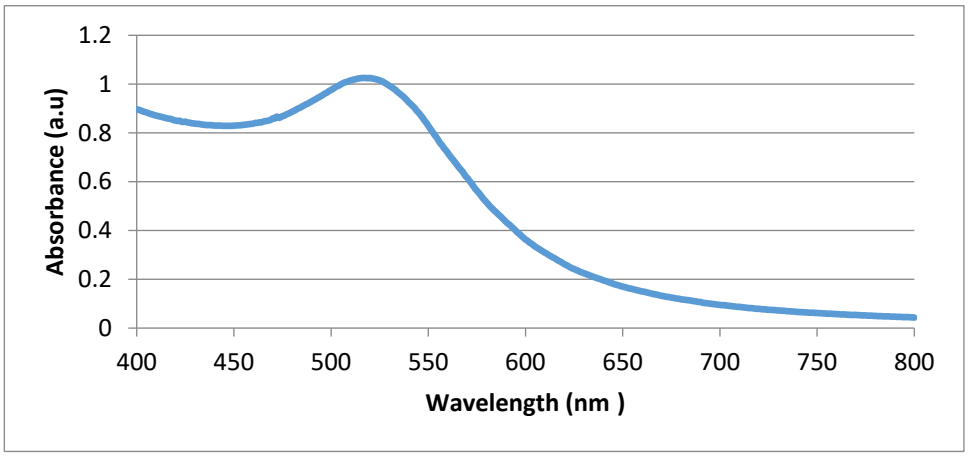

Figure 12 Plain Au visible light absorption.

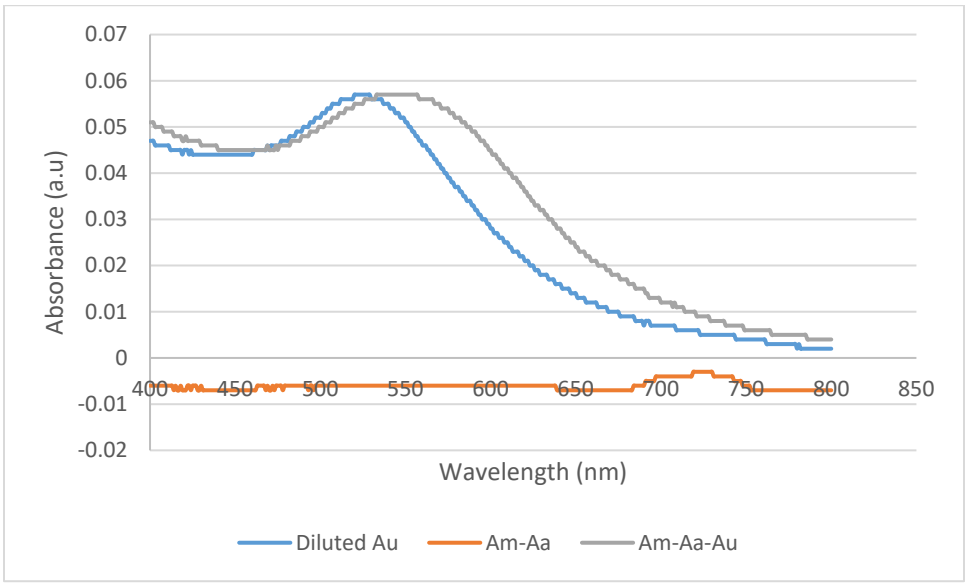

Figure 13 Visible light absorption analysis. Am-Aa (Plain monomers), diluted Au (250 μL Au+6mL nanopore water) and Am-Aa-Au (0.5gAm+0.5gAa+250 μL Au).

4.4 Swelling and deswelling assessment

Hydrogel swelling phenomena occur by difference in osmotic pressure that is causing water molecules to diffuse into its matrix. This can be controlled by the copolymer nature such as, degree of cross-linking, polymer-solvent interaction and functional groups charge density. Also, it can be driven by environmental conditions such as RH%, temperature and pH. Since the proposed hydrogel will be applied in atmospheric water recovery and it will be exposed into sunlight and RH(%), its swelling temperature were figured out by placing it in a furnace at different temperature and constant RH(%) range. According to Table 8 and Figure 16, the hydrogel shows positive temperature-sensitive behavior where, swelling is more predominant at relatively high temperatures ranges from 20-70ºC and above that the hydrogel will start deswelling. This advantage enables the hydrogel water recovery regardless of the region for example arid or semi-arid regions because these regions undergo relatively high temperatures when compared to normal regions. This swelling and deswelling behavior is resulting from the USCT where, out of its swelling range the hydrodynamic radius is decreasing because hydrogen bonding is holding the monomers and causing the hydrogel to squeeze the absorbed water. In this synthesis method, we accomplish a thermo-responsive hydrogel that makes it applicable for atmospheric water recovery because it swells under wide temperature range [20-70ºC] which makes it suitable for this type of application regardless of the region. In this research, the swelling percentage will be calculated by using the expression below [38].

$$= \frac{Weight_{wet} - Weight_{dry}}{Weight_{dry}} * 100 \quad (3)$$

Table 6 Plain hydrogels swelling behavior under different temperatures. T_1= [20-30]ºC, T_2= [30-40]ºC, T_3= [40-50]ºC, T_4= [50-60]ºC, T_5= [60-70]ºC..

		P(Am-co-Aa)					
		Weight (g)			Swelling (%) (3)		
Temperature (c)	Time (hours)	Sample 1	Sample 2	Sample 3	Sample 1	Sample 2	Sample 3
20-30	0	0.6200	0.2786	0.2515	0	0	0
20-30	1	0.6330	0.286	0.2602	2	3	3
30-40	2	0.6455	0.2885	0.2609	4	4	4
40-50	3	0.6548	0.2992	0.2732	6	7	9
50-60	4	0.6621	0.3002	0.2756	7	8	10
60-70	5	0.6701	0.312	0.2848	8	12	13

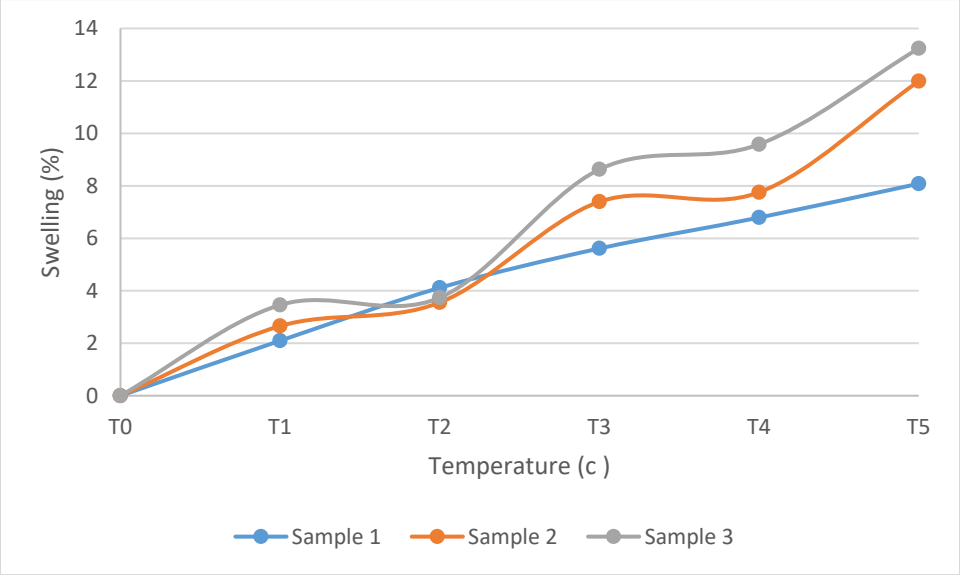

Figure 14 Plain hydrogels swelling behavior under different temperatures. T_1= [20-30]ºC, T_2= [30-40]ºC, T_3= [40-50]ºC, T_4= [50-60]ºC, T_5= [60-70]ºC.

Table 7 Modified hydrogels swelling behavior under different temperatures. T_1= [20-30]ºC, T_2= [30-40]ºC, T_3= [40-50]ºC, T_4= [50-60]ºC, T_5= [60-70]ºC.

		P(Am-co-Aa)/Au					
		Weight (g)			Swelling (%) (3)		
Temperature (c)	Time (hours)	Sample 1	Sample 2	Sample 3	Sample 1	Sample 2	Sample 3
20-30	0	0.6357	0.1746	0.3237	0	0	0
20-30	1	0.6462	0.1819	0.3326	2	4	3
30-40	2	0.6540	0.1836	0.3340	3	5	3
40-50	3	0.6664	0.1901	0.3480	5	9	8
50-60	4	0.6732	0.1915	0.3492	6	10	8
60-70	5	0.6829	0.2039	0.3628	7	17	12

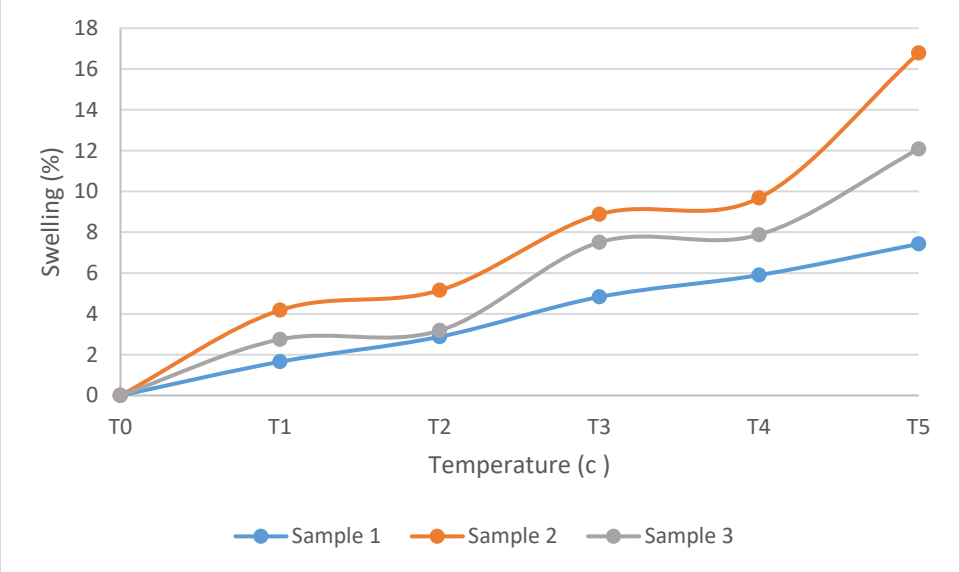

Figure 15. Modified hydrogels Swelling Temperature. T_1= [20-30]ºC, T_2= [30-40]ºC, T_3= [40-50]ºC, T_4= [50-60]ºC, T_5= [60-70]ºC.

Table 8 Modified and plain hydrogels average swelling temperature. T_1= [20-30]ºC, T_2= [30-40]ºC, T_3= [40-50]ºC, T_4= [50-60]ºC, T_5= [60-70]ºC..

		P(Am-co-Aa)	P(Am-co-Aa)/Au
Temperature (c)	Time (hours)	Average Swelling (%)	
20-30	0	0	0
20-30	1	3	3
30-40	2	4	4
40-50	3	7	7
50-60	4	8	8
60-70	5	11	12

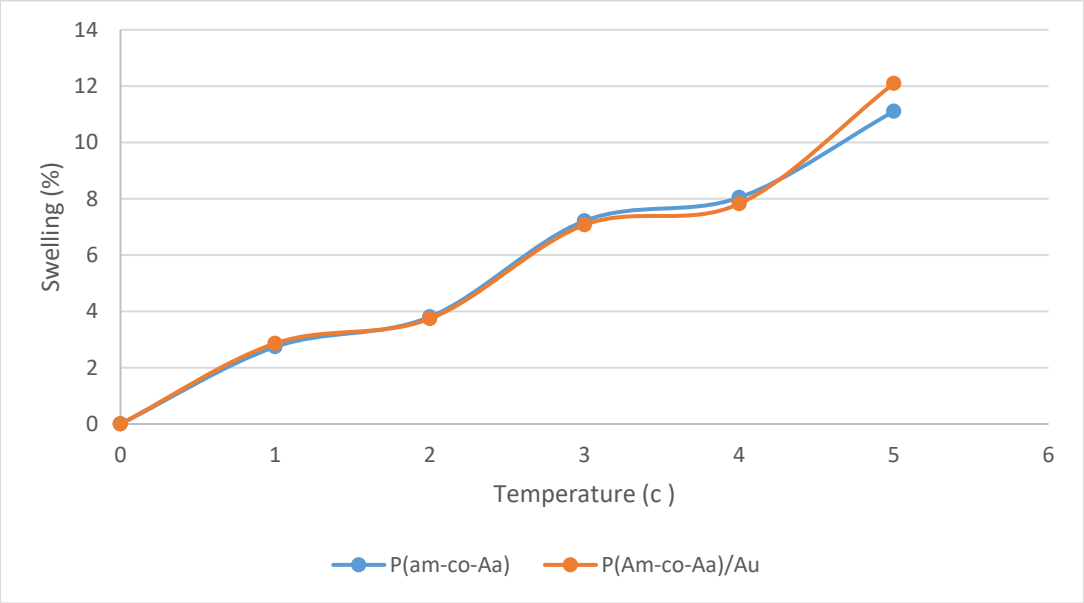

Figure 16 Modified and plain hydrogels average swelling temperature. T_1= [20-30]ºC, T_2= [30-40]ºC, T_3= [40-50]ºC, T_4= [50-60]ºC, T_5= [60-70]ºC.

In general, a hydrogel swells more in liquid water than in vapor water because the more monomer ionization caused by water molecules. To ensure that the hydrogel expose good hydrophilic properties, its swelling behavior were investigated in nanopure water (pH=7) for 5 hours under a swelling temperature [20-30ºC]. According to Table 9 and Figure 17, the hydrogel average swelling (%) after five hours is about 3541% (see appendix) indicating good hydrophilic properties. This can be explained by monomers increased electrostatic repulsion because when pH is neutral, the majority of amines and carboxylic groups are ionized because pH is above the pK_a of carboxylic group and below the pK_b of amines group [36, 43].

Table 9 . P(Am-co-Aa)/Au hydrogel soaked in nanopure water.

	P(Am-co-Aa)					
	Weight (g)			Swelling (%) (3)		
Time (hours)	Sample 1	Sample 2	Sample 3	Sample 1	Sample 2	Sample 3
0	0.3422	0.1989	0.0932	0	0	0
1	3.124	2.4517	0.9831	813	1133	955
2	5.3662	4.0784	1.7802	1468	1950	1810
3	8.3961	5.5188	2.4848	2354	2675	2566
4	10.2056	6.6253	2.9972	2882	3231	3116
5	12.2744	7.4087	3.3662	3487	3625	3512

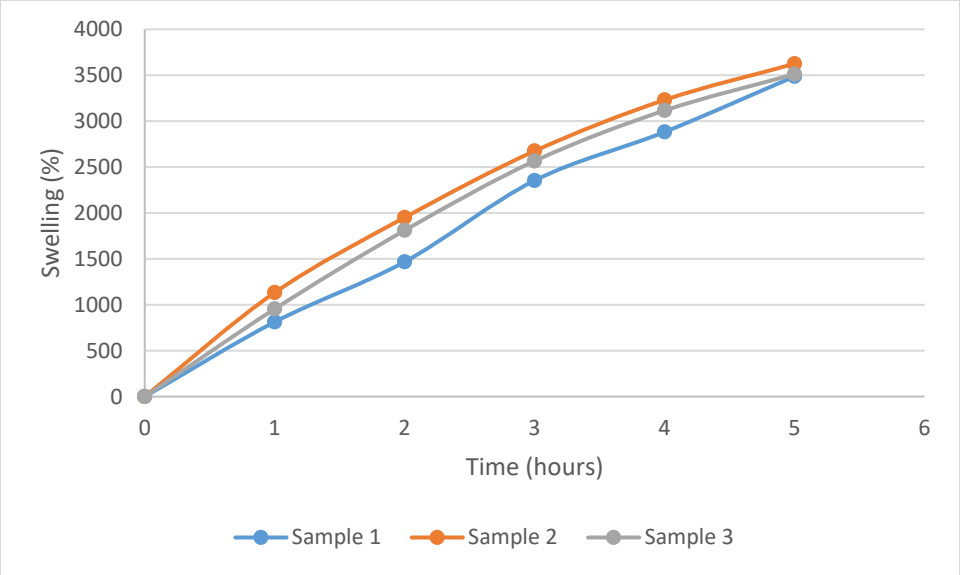

Figure 17. P(Am-Co-Aa)/Au hydrogel soaked in water.

When the moisture content surrounding the hydrogel is decreased, less swelling is achieved by the hydrogel because less osmotic pressure between the hydrogel and surroundings. However, our proposed hydrogel still absorb water when its expose for 5 hours to RH (%) as low as [20-30], the plain hydrogel achieves swelling value of about 0.04% (Table 10) and the hydrogel loaded with salt absorb 1.8% (Table 13) water vapor. Whereas, when the plain hydrogel undergoes RH (%) between [80-90] its swelling increase to 23.7% (Table 12) and further increase to approximately 27% for the hydrogel loaded with salt because more electrostatic repulsion caused by $CaCl_2$ (Table 15). A summary of the water vapor swelling capacity is shown in Figure 18 and Figure 19.

Table 10 P(Am-co-Aa) swelling with time at RH(%)[20-30] and constant temperature.

Time (hours)	Weight (g)	Swelling (%) (3)
0	1.1300	0.000
1	1.1301	0.009
2	1.1302	0.018
3	1.1303	0.027
4	1.1303	0.027
5	1.1305	0.044

Table 11 P(Am-co-Aa) swelling with time at RH(%)[50-60] and constant temperature.

Time (hours)	Weight (g)	Swelling (%) (3)
0	1.1690	0.0
1	1.2063	3.2
2	1.2071	3.3
3	1.2352	5.7
4	1.2652	8.2
5	1.3184	12.8

Table 12 . P(Am-co-Aa) swelling with time at RH(%)[80-90] and constant temperature.

Time (hours)	Weight (g)	Swelling (%) (3)
0	1.1223	0.0
1	1.1910	6.1
2	1.2946	15.4
3	1.3625	21.4
4	1.3828	23.2
5	1.3888	23.7

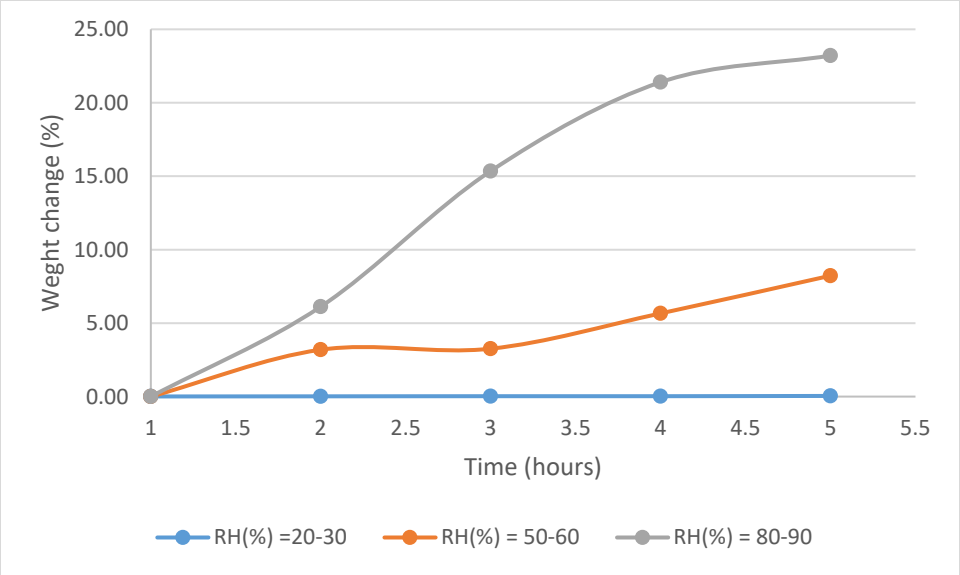

Figure 18. P(Am-co-Aa) swelling with time at different RH and constant temperature**.**

Table 13. P(Am-co-Aa)/Au/$CaCl_2$ swelling with time at RH[20-30] and constant temperature.

Time (hours)	**Weight (g)**	**Swelling (%) (3)**
0	4.4306	0.0
1	4.4557	0.6
2	4.4711	0.9
3	4.4818	1.2
4	4.4960	1.5
5	4.5116	1.8

Table 14. P(Am-co-Aa)/Au/$CaCl_2$ swelling with time at RH(%)[50-60] and constant temperature.

Time (hours)	**Weight (g)**	**Swelling (%) (3)**
0	4.4080	0.0
1	4.6103	4.6
2	4.7715	8.2
3	4.9101	11.4
4	5.0173	13.8
5	5.1478	16.8

Table 15. P(Am-co-Aa)/Au/$CaCl_2$ swelling with time at RH(%)[80-90] and constant temperature.

Time (hours)	Weight (g)	Swelling (%) (3)
0	4.4080	0.0
1	4.8799	10.7
2	5.1291	16.4
3	5.2455	19.0
4	5.4046	22.6
5	5.6121	27.3

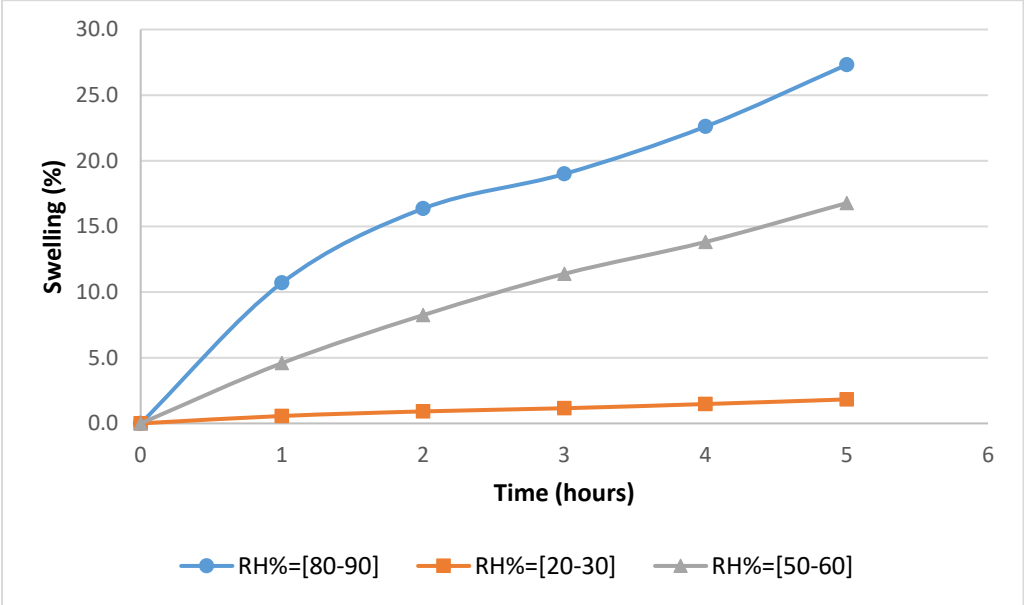

Figure 19. P(Am-co-Aa)/Au/$CaCl_2$ swelling with time at different RH and constant temperature.

CHAPTER 5 FIELD CAMPAIGN

5.1 Controlled structure

The controlled structure may provide the hydrogel with the appropriate environment for swelling and deswelling accomplishing an Atmospheric Water Generator (AWG) for potable water recovery. It's consisted of glass lidded pyrex were small portion of the lid was cut and substituted with an active heat sink to encourage heat dissipation (Figure 20.1, Figure 20.2 and Figure 20.3). Also, the AWG will be sealed perfectly with 100% silicon sealant to prevent any kind of leaking and insulated from the top with aluminum tape to aim in sunlight reflection (Figure 20.4 and Figure 20.5) however, there will be small portion from the top that is not insulated to allow small portion for sunlight entrance causing hydrogel deswelling (Figure 20.6). The hydrogel will be placed on an insulated foam that is stabilized perfectly and located 10 cm from the light source.

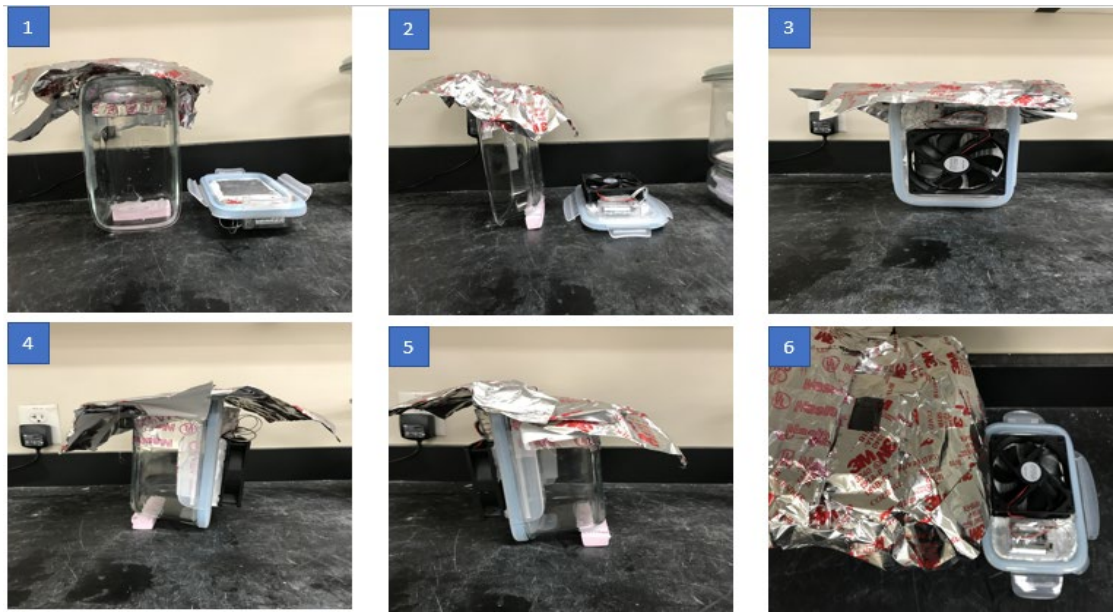

Figure 20. Control structure parts explanation, 1) Opened AWG front. 2) Opened AWG side. 3) Connected AWG front. 4) Connected AWG side. 5) Connected AWG side. 6) Connected AWG top.

The outdoor AWG assembly will be as follow. In the evening, the AWG will be opened to allow the hydrogel swelling and this can be achieved by the functional group and the deliquescent salt hydrophilic properties. In the morning, the AWG will be closed to allow water recovery and this can be achieved by the visible sunlight absorption caused by the addition of Au-Np's that will force the hydrogel to deswell along with the salt loaded inside and outside the hydrogel matrix and this can be achieved by the first law of thermodynamic. In our system, the water inside and outside the hydrogel will be evaporated with the aim of sunlight because the absorbed energy by liquid water when it is exposed to enough heat which allow water molecules to change their state from liquid to vapor. After that, water droplet will be induced through constant formation of hydrogen bonds because water vapor will release its energy in form of heat on the aluminum active heat sink and it converts into liquid water.

5.2 Outdoor pilot study

Due to the weather fluctuations at UCF in November 2019, a pilot study was performed at UCF engineering 1 lab number 438 to assess an approximate behavior of the hydrogel water vapor swelling and deswelling. UCF campus have an average night-time temperature range [20-30^{o}C] and RH range [70-80%]. This was simulated by placing the hydrogel for 12 hours in a furnace under temperature ranges from [20-30^{o}C] and at RH range [70-80%] simulating the night-time weather at UCF campus. After allowing the hydrogel to swell, it achieves an average swelling value of 54% after 12 hours (Table 16). Then, deswelling test was simulated under artificial sunlight using lightbulb. The sunlight was simulated in accordance to the National Aeronautics and Space Administration (NASA), they claim that the intensity of sunlight is 1,367 Watts/m^2 [44]. Therefore, when the hydrogel is placed under known lightbulb watts (200 Watts) with

considering the hydrogel to lightbulb distance (10cm), the hydrogel will undergo an intensity of 1,367 Watts/m^2 (see Figure 21 and appendix calculations).

Figure 21. Deswelling test and sunlight simulation.

After preforming these tests, the hydrogel was placed in the AWG for 2.5 hours. The water recovered by 4.4406g hydrogel was 1.9358g of water when it was exposed to water vapor for 12 hours (see Figure 23, Table 17). The hydrogel provides a better deswelling performance under sunlight when compared to commercially available dehumidifiers such as Zeolite that requires a temperature of 350ºC to start deswelling [45]. Also, activated alumina that require a temperature of 290 ºC to start deswelling [46]. Furthermore, silica gel that requires a temperature between [85-100 ºC] to start deswelling [47] (see Table 21). The proposed hydrogel deswell 71% of the absorbed water when it's under artificial sunlight exposure. Currently, the amount to recover the achieved water quantity will cost $ 7 (see Table 23). This cost of the hydrogel can be reduced if we obtain the salt from the wasted by-products in RO process that is known as the concentrated water that contain a huge amount of total dissolved solids.

Overall, the synthesized product shows a positive temperature-sensitive hydrogel Figure 16. For water recovery, I just did 12 hours swelling experiment for the hydrogel loaded with salt (Table 17). After that, the same hydrogel was placed in the AWG and went through deswelling

experiment for 2.5 hours using simulated sunlight. Then, the amount of recovered water was measured from this experiment 1.9358g when 4.4406g hydrogel is exposed to 1,367 Watts/m^2 light intensity for 2.5 hours (Figure 21 and Figure 23). Hydrogel cost effectiveness analysis is shown in Table 23. Our AWG recover 68% of the absorbed water 2.5 hours (see Table 22Table 20) whereas in [22], their AWG recover 54% of the absorbed water undergoing the same time and temperature conditions. In 2.5 hour the proposed hydrogel deswell 71% of the water absorbed in 12 hours.

Table 16 Pilot test swelling data. (Trail 1)

Time (hours)	**Weight (g)**	**Swelling (%) (3)**
0	4.4150	0
2	5.0994	16
4	5.3423	21
6	5.5144	25
8	5.8013	31
10	6.0972	38
12	6.3709	44

Table 17 Pilot test swelling data (Trail 2)

Time (hours)	**Weight (g)**	**Swelling (%) (3)**
0	4.4406	0
2	5.8358	31
4	5.9371	34
6	6.1946	40
8	6.5144	47
10	6.8474	54
12	7.2604	63

Table 18 Pilot test swelling data (Trail 3)

Time (hours)	Weight (g)	Swelling (%) (3)
0	4.4278	0
2	4.9676	12
4	5.6397	27
6	5.8545	32
8	6.1578	39
10	6.4723	46
12	6.8156	54

Table 19 Pilot test swelling data (Trail 1, 2 &3 average)

Time (hours)	Weight (g)	Swelling (%) (3)
0	4.4278	0
2	5.3009	20
4	5.6397	27
6	5.8545	32
8	6.1578	39
10	6.4723	46
12	6.8156	54

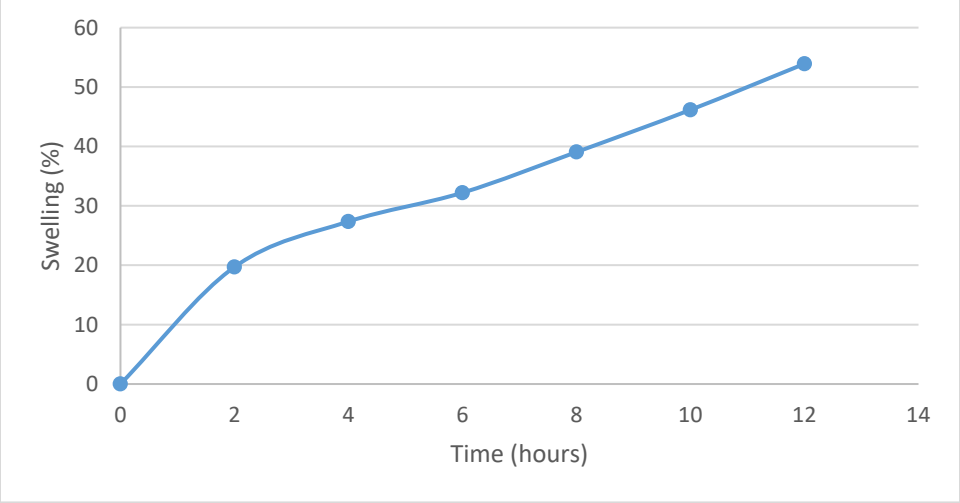

Figure 22 Average hydrogel swelling in 12 hours RH%[70-80].

Table 20 Hydrogel under artificial sunlight (Trail 2).

Hydrogel	Weight (g)	Calculations
After 2.5 hours	5.2443	Measured
Water desorption after 2.5	2.0161	7.2604-5.2773
Water absorbed in 12 hours	2.8198	7.2604-4.4406
Water recovered by aluminum plate	1.9358	Measured

Table 21. Hydrogel deswelling comparison with commercial dehumidifiers

Dehumidifier	Deswelling Temperature (c)	Source
P(Am-co-Aa)/Au/$CaCl_2$	Artificial sunlight	This work
P(Am)/CNT/$CaCl_2$	Normal sunlight	[22]
Zeolite	350	[45]
Activated alumina	290	[46]
Silica gel	[85-100]	[47]

Table 22 Water recovery comparison

	P(Am-co-Aa)/Au/$CaCl_2$	**P(Am)/CNT/$CaCl_2$**
Hydrogel dry weight (g)	4.4406	35
Water absorbed (g)	2.8198	37
Absorption time (hours)	12	17
Water desorbed (g)	2.0161	-
Water recovered (g)	1.9358	20
Water recovered per dry unit hydrogel (%)	43	57
Water recovered per water absorbed (%)	68	54
Water desorbed in 2.5 hours per water absorbed in 12 hours (%)	71	-
Source	This work	[22]

Figure 23 Recovered water.

Table 23. Hydrogel cost effectiveness analysis

Chemical supplied by SigmaAldrich	Price and quantity ($/weight)	Price for 1 gram hydrogel ($/weight)
Acrylamide	$\frac{60.50}{100\ g}$	0.3025
Acrylic Acid	$\frac{46.10}{500g}$	0.0461
Potassium persulfate	$\frac{15.64}{25g}$	0.003128
N,N'-Methylenebis(acrylamide)	$\frac{39.60}{100mL}$	0.015048
N,N,N'N'-Tetramethylenediamine	$\frac{70}{100mL}$	0.0175
Gold nanoparticles	$\frac{368}{100mL}$	0.092
Calcium chloride	$\frac{40.70}{25g}$	6.512
		Total=7

CHAPTER 6 CONCLUSION

6.1 Final remarks

Atmospheric water recovery is an important topic and currently immerging technology having border range of ambiance. It can be accomplished using a combination of nano and bio-technology with applying the principles of b^3p. In summary, we synthesized an existing type of polymers using different polymerization techniques, free radical copolymerizations that result in a human-friendly, thermo-sensitive, and hydrophilic copolymer. Theoretically and based on current literatures, these types of hydrogels can be used in pharmaceutical purposes therefore can be safely consumed by humans. Au-Np's were successfully loaded inside the hydrogel, this was proved using the characterization methods mentioned in this research. The hydrogel shows high swelling potential resulted from a strong internal electrostatic repulsion. The result obtained expose that P(Am-co-Aa)/Au-Np's/$CaCl_2$ accomplishes an extensive swelling behavior in water vapor, about 2g of potable water in 12 hours under RH% [70-80] and it releases 71% of that water when exposed to an artificial sunlight for 2.5 hours. The AWG recover 68% of the water absorbed by the hydrogel.

6.2 Recommendations

The following are recommendations for future investigation

(1) Testing the hydrogel under different RH% and T using manual controlled furnace is quite time consuming. In the future, I would like to recommend using an automatic furnace control such as NETZSCH Jupiter simultaneous thermal analyzer 449 combined with water vapor generator.

(2) Test the hydrogel salt loading under different salt concentration and different kind of salts

(3) test the hydrogel swelling behavior under different cross-linking density and different monomer ratios.

(4) Bacteria growth environment is moist and warm environment. Therefore, testing their growth inside the AWG is important.

(5) Testing the hydrogel deswelling behavior under different sunlight intensity.

APPENDIX: SAMPLE CALCULATIONS

Swelling and deswelling calculations (3) (Table 6**)**

$$\text{Swelling (\%)} = \frac{0.6701 - 0.6200}{0.6200} * 100 = 8\%$$

P(Am-co-Aa)/Au swelling (%) average after 5 hours in nanopore water (Table 9**)**

$$\text{Average} = \frac{3487 + 3625 + 3512}{3} = 3541\%$$

Sunlight simulation calculations

$$\text{intensity} = \frac{light\ bulb\ watts}{sphere\ surface\ area} = \frac{200\ W}{4\pi\ r^2} = \frac{200\ W}{4\pi\ (0.1m)^2} = 1{,}367\ \text{W/m}^2$$

Hydrogel cost calculations (Table 23 **)**

$\text{Am} = \frac{\$60.50}{100g} * 0.5g =$	\$0.3025
$\text{Aa} = \frac{\$46.10}{500g} * 0.5g =$	\$0.0461
$\text{KPS} = \frac{\$15.64}{25000mg} * 5mg =$	\$0.003128
$\text{MBAA} = \frac{\$39.60}{1000mg} * 0.38mg =$	\$0.015048
$\text{TEMED} = \frac{\$70}{100000\mu L} * 25\ \mu L =$	\$0.0175
$\text{Au-Np's} = \frac{\$368}{100000\mu L} * 250\ \mu L =$	\$0.092
$\text{Am} = \frac{\$40.70}{25g} * 4g =$	\$6.512
	Total=\$7.0

LIST OF REFERENCES

1. Affairs, U.N.D.o.E.a.S. *Water Scarcity* 2018, December 12; Available from: https://www.un.org/waterforlifedecade/scarcity.shtml.
2. Survey, U.S.G. *Where is Earth's Water?* 2018, December 2018; Available from: https://www.usgs.gov/special-topic/water-science-school/science/where-earths-water?qt-science_center_objects=0#qt-science_center_objects.
3. District's, S.F.W.M. *Desalination in South Florida – Frequently Asked Questions*. 2018, December 12 Available from: https://www.sfwmd.gov/sites/default/files/documents/desal_faqs.pdf.
4. Wood, L.A.J.J.o.R.o.t.N.B.o.S.C.E. and I. C, *The use of dew-point temperature in humidity calculations.* 1970. **74**: p. 117-122.
5. UNIVERSITY, F.S. *FLORIDA CLIMATE CENTER*. 2018, December 12; Available from: https://climatecenter.fsu.edu/products-services/data/other-normals/relative-humidity.
6. Buchholz, F.L.J.J.o.c.e., *Superabsorbent polymers: an idea whose time has come.* 1996. **73**(6): p. 512.
7. Young, R.J. and P.A. Lovell, *Introduction to polymers*. 2011: CRC press.
8. Flory, P.J., *Principles of polymer chemistry*. 1953: Cornell University Press.
9. Qiu, Y. and K.J.A.d.d.r. Park, *Environment-sensitive hydrogels for drug delivery.* 2001. **53**(3): p. 321-339.
10. Lobo, A.O., et al., *Fast functionalization of vertically aligned multiwalled carbon nanotubes using oxygen plasma.* 2012. **70**: p. 89-93.
11. Pinheiro, R.A., et al., *Water vapor condensation and collection by super-hydrophilic and super-hydrophobic VACNTs.* 2018. **87**: p. 43-49.
12. Das, R., B.F. Leo, and F.J.N.r.l. Murphy, *The toxic truth about carbon nanotubes in water purification: a perspective view.* 2018. **13**(1): p. 183.
13. Bellucci, S., *Carbon nanotubes toxicity*, in *Nanoparticles and Nanodevices in Biological Applications*. 2009, Springer. p. 47-67.
14. Nilsson, T., et al., *Condensation of water by radiative cooling.* 1994. **5**(1-4): p. 310-317.
15. Zheng, Y., et al., *Directional water collection on wetted spider silk.* 2010. **463**(7281): p. 640.
16. Somenath Mitra, S.R., *Carbon nanotube immobilized super-absorbing membranes*. 2016.
17. Shamaila, S., et al., *Gold nanoparticles: an efficient antimicrobial agent against enteric bacterial human pathogen.* 2016. **6**(4): p. 71.
18. Sershen, S., et al., *Temperature-sensitive polymer–nanoshell composites for photothermally modulated drug delivery.* 2000. **51**(3): p. 293-298.

19. Echeverria, C. and C.J.M.r.c. Mijangos, *Effect of gold nanoparticles on the thermosensitivity, morphology, and optical properties of poly (acrylamide–acrylic acid) microgels.* 2010. **31**(1): p. 54-58.

20. Furukawa, H., et al., *Water adsorption in porous metal–organic frameworks and related materials.* 2014. **136**(11): p. 4369-4381.

21. Byun, Y. and A.J.A.C.I.E. Coskun, *Epoxy-Functionalized Porous Organic Polymers via the Diels–Alder Cycloaddition Reaction for Atmospheric Water Capture.* 2018. **57**(12): p. 3173-3177.

22. Li, R., et al., *Hybrid hydrogel with high water vapor harvesting capacity for deployable solar-driven atmospheric water generator.* 2018. **52**(19): p. 11367-11377.

23. Sanchez, C., H. Arribart, and M.M.G.J.N.m. Guille, *Biomimetism and bioinspiration as tools for the design of innovative materials and systems.* 2005. **4**(4): p. 277.

24. Jamsari, E.A., et al., *Ibn Firnas and his contribution to the aviation technology of the world.* 2013. **7**(1): p. 74-78.

25. Darder, M., P. Aranda, and E.J.A.M. Ruiz-Hitzky, *Bionanocomposites: a new concept of ecological, bioinspired, and functional hybrid materials.* 2007. **19**(10): p. 1309-1319.

26. Tracy, C.R., K.A. Christian, and C.R.J.E. Tracy, *Not just small, wet, and cold: effects of body size and skin resistance on thermoregulation and arboreality of frogs.* 2010. **91**(5): p. 1477-1484.

27. Tracy, C.R., N. Laurence, and K.A.J.T.A.N. Christian, *Condensation onto the skin as a means for water gain by tree frogs in tropical Australia.* 2011. **178**(4): p. 553-558.

28. Halliday, T., *The book of frogs: A life-size guide to six hundred species from around the world*. 2016: University of Chicago Press.

29. Toledo, R., C.J.C.B. Jared, and P.P.A. Physiology, *Cutaneous adaptations to water balance in amphibians.* 1993. **105**(4): p. 593-608.

30. Tracy, C.R., et al., *Thermal and hydric implications of diurnal activity by a small tropical frog during the dry season.* 2013. **38**(4): p. 476-483.

31. Tracy, C.R., K.A.J.P. Christian, and B. Zoology, *Preferred temperature correlates with evaporative water loss in hylid frogs from northern Australia.* 2005. **78**(5): p. 839-846.

32. Blaylock, L.A., R. Ruibal, and K.J.C. Platt-Aloia, *Skin structure and wiping behavior of phyllomedusine frogs.* 1976: p. 283-295.

33. UÇAR, İ.O. and H.Y.J.T.J.o.C. ERBİL, *Droplet condensation on polymer surfaces: A review.* 2013. **37**(4): p. 643-674.

34. Zhai, L., et al., *Patterned superhydrophobic surfaces: toward a synthetic mimic of the Namib Desert beetle.* 2006. **6**(6): p. 1213-1217.

35. Comanns, P.J.J.o.E.B., *Passive water collection with the integument: mechanisms and their biomimetic potential.* 2018. **221**(10): p. jeb153130.

36. Erceg, T., et al., *The influence of synthesis parameters on swelling behaviour of pH-sensitive acrylate based hydrogels.* 2017. **58**(4): p. 433-444.

37. Tomar, R.S., et al., *Synthesis of poly (acrylamide-co-acrylic acid) based superabsorbent hydrogels: Study of network parameters and swelling behaviour.* 2007. **46**(5): p. 481-488.

38. Nesrinne, S. and A.J.A.J.o.C. Djamel, *Synthesis, characterization and rheological behavior of pH sensitive poly (acrylamide-co-acrylic acid) hydrogels.* 2017. **10**(4): p. 539-547.

39. Bai, J., et al., *One-pot synthesis of polyacrylamide-gold nanocomposite.* 2007. **106**(2-3): p. 412-415.

40. Jans, H., et al., *Poly (acrylic acid)-stabilized colloidal gold nanoparticles: synthesis and properties.* 2010. **21**(45): p. 455702.

41. Mandapalli, P.K., et al., *Polymer–gold nanoparticle composite films for topical application: Evaluation of physical properties and antibacterial activity.* 2017. **38**(12): p. 2829-2840.

42. Gaabour, L.J.R.i.p., *Spectroscopic and thermal analysis of polyacrylamide/chitosan (PAM/CS) blend loaded by gold nanoparticles.* 2017. **7**: p. 2153-2158.

43. Atta, A.M., et al., *Fast responsive poly (acrylic acid-co-N-isopropyl acrylamide) hydrogels based on new crosslinker.* 2009. **112**(1): p. 114-122.

44. Administration, N.A.a.S. *The Inconstant Sun*. 2019 July 24; Available from: https://science.nasa.gov/science-news/science-at-nasa/2003/17jan_solcon.

45. Sayılgan, Ş.Ç., et al., *Effect of regeneration temperature on adsorption equilibria and mass diffusivity of zeolite 13x-water pair.* 2016. **224**: p. 9-16.

46. Serbezov, A.J.J.o.C. and E. Data, *Adsorption equilibrium of water vapor on F-200 activated alumina.* 2003. **48**(2): p. 421-425.

47. Chua, H., et al., *Transient modeling of a two-bed silica gel–water adsorption chiller.* 2004. **47**(4): p. 659-669.